JOURNAL OF MECHANICAL ENGINEERING AND SCIENCES (JMES)
ISSN: 2289-4659 e-ISSN: 2231-8380
VOL. 15, ISSUE 2, 8082 – 8094
DOI: https://doi.org/10.15282/jmes.15.2.2021.12.0637

ORIGINAL ARTICLE

Magnetohydrodynamic peristaltic flow of Bingham fluid in a channel: An application to blood flow

C. Rajashekhar[1], G. Manjunatha[2], F. Mebarek-Oudina[3], Hanumesh Vaidya[4,*], K.V. Prasad [4], K. Vajravelu[5], A.Wakif[6]

[1] Department of Mathematics, Karnataka State Akkamahadevi Women's University, Vijayapura 586108, Karnataka, INDIA
[2] Department of Mathematics, Manipal Institute of Technology, Manipal Academy of Higher Education, Manipal 576104, Karnataka, INDIA
[3] Department of Physics, Faculty of Sciences, University of 20août 1955-Skikda, Skikda 21000, ALGERIA
[4] Department of Mathematics, Vijayanagara Sri Krishnadevaraya University, Ballari 583105, Karnataka, INDIA
[5] Department of Mathematics, University of Central Florida, Orlando FL 32816, USA
[6] Laboratory of Mechanics, Faculty of Sciences Aïn Chock, Hassan II University, B.P. 5366 Mâarif, Casablanca 20000, MOROCCO

ABSTRACT – The paper examined a theoretical investigation of the stimulus of mass and heat transfer on the channel's peristaltic utilization of the MHD Bingham liquid. The research study is motivated to explore blood circulation in the little vessels by taking the slip, variable thermal conductivity, and thickness of the wall features into account. The leading constitutive equations are established based on low Reynolds number and approximations for long wavelengths. The solution for the resulting nonlinear energy and momentum equations is obtained using a semi-analytic method, while the exact solution for the concentration field is obtained. Using the MATLAB software, the influences of different constraints on the interest of physiological quantities are represented graphically. One of the considerable outcomes of the current model exposes that the existence of variable fluid properties boosts the rate as well as temperature level areas. The rheological and flow properties of various biological fluids can be derived from this model as a particular case. Moreover, the formation of stuck bolus diminishes for larger values of the magnetic and velocity slip constraints.

ARTICLE HISTORY
Received: 03rd Oct 2019
Revised: 13th Sept 2020
Accepted: 22nd Oct 2020

KEYWORDS
Thermal Slip;
velocity Slip;
concentration slip;
wall rigidity;
wall elasticity

INTRODUCTION

Peristaltic flow is a mechanism in which the flow is induced by the shriveling and spreading out of the distensible tube wall, which results in a sinusoidal wave-like movement. This mechanism plays an essential function in the development of lots of organic liquids such as in the circulation of diet bolus with the esophagus, the activity of chyme in the stomach system, the vasomotion of blood in tiny arteries and also several various other such procedures required for the appropriate performance of organic liquids. The initial study on the peristaltic mechanism was initiated by Latham [1] for investigating the flow of urine through the ureter. The very early research studies on the peristaltic circulation have been lugged out with the fluids such as Newtonian. The usage of non-Newtonian liquids is of higher relevance from a biological standpoint of view, as many physical liquids display non-Newtonian actions. Motivated by this, Raju and Devanathan [2] used the fluid of non-Newtonian to study the mechanism of peristalsis. Their exploration has unbolted a large door in the study of non-Newtonian fluid peristaltic transportation. Subsequently, several researchers investigated the peristalsis by taking non-Newtonian fluids in different geometries and configurations [3–6].

The early peristaltic flow investigations were conducted in the non-appearance of a magnetic field. However, the presence of red blood cells in the blood composition influences the magnetic field's use in the study of the blood's peristaltic mechanism. Bloodstream was revealed to characterize a mathematical model with a shear rate below 100 for the magentohydrodynamic (MHD) flow. The transportation of the peristaltic flow of a liquid along with the MHD factors in a tube/channel assists in clearing up problems regarding the advancement of bodily liquids, the procedure of bloodstream pump makers, expedition on the occupied of a peristaltic MHD blower, etc. In both natural and mechanical applications [7–15], the inspiration of the magnetic field (MF) on peristalsis of non-Newtonian fluid accounting slip conditions has been explored. Guo et al. [16] studied Jeffrey fluid's peristaltic MHD flow through a permeable channel. Furthermore, Hayat et al. [17] studied the stimulus of Soret and Dufour on the Prandtl fluid's peristaltic MHD movement through a rotating channel. The impacts of convective limit conditions on Jeffery nanofluid's peristaltic MHD system in a bowed channel was numerically reconnoitered by Tanveer et al. [18]. Kumar et al. [19] examined the influence of heat transfer through a change heat source on the Powell-Eyring MHD fluid. Manjunatha et al. [20] recently looked at the impacts of slip and magnetohydrodynamics on Jeffrey fluid by a constant channel.

The influence of slip conditions on the walls, combined with mass and heat exchange, has major applications in blood oxygenation and hemodialysis. It is seen that the no-slip conditions on the governing equations of motion and energy of natural fluids fail to provide a better estimation of peristaltic action uncovered in different biological systems. The applicability of slip conditions at the wall can be observed in the cleaning of an artificial heart. Wall properties is another significant property that grabbed the consideration of numerous researchers in the last decade because of their applications

*CORRESPONDING AUTHOR | Hanumesh Vaidya | ✉ hanumeshvaidya@gmail.com

to health science. An extensive study on considering these two properties is available in [21–30]. Most of the investigations on the peristaltic flow have been carried out by taking constant thermophysical properties. However, there is ample proof in the literature that the fluid's viscosity differs concerning the wall thickness [31]–[33], and thermal conductivity differs for temperature [34, 35]. Owing to the composite action of the blood, the different rheological impacts like variable viscosity, shear rate, hematocrit, etc., are difficult to describe. Thus, there is an enormous way to describe these equations; more or less use curve fitting to experimental and discrete data along the others are based on specific rheological models. In [36–40], the use of the Bingham model in scrutinizing the peristaltic scheme through various geometries is recently reported midst the several models of non-Newtonian.

This study consist of the deviation of variable fluid properties on the peristaltic flow of an MHD Bingham fluid that has not been considered so far. The present research investigates the MHD flow in a uniform channel comprising peristaltic blood (PB). Blood is modeled as a Bingham fluid to take accounts of slip, wall, and variable fluid properties. The examination and consequences of the investigation are particularly appropriate in the pathological state for the transport of PB in small-dimensional coronary veins. Further, the analysis tolerates the guarantee of multifold essential applications in the domain of physiological fluid elements. In some instances, evaluations of an array of liquid mechanical factors are needed when any physiological liquid needs to bear slip effects near the walls. Likewise, the examination will have an essential manner in inspecting the stream in a vessel when the endothelial layer of the luminal surface relates to glycocalyx, which contains an arrangement of small-scale atoms and squeezed plasma proteins. In addition to all this, the analysis should find its applications in developing heart-lung machines and dialysis machines. Since very few articles in their formulation have addressed the variable liquid properties, this paper will close the distance by observing the liquid to demonstrate these features. The authors also endeavored to make a mathematical model which provides practical blood flow manifestations in tiny arteries.

FORMULATION OF THE PROBLEM

Consider the non-Newtonian 2D flow of an incompressible fluid with changing fluid characteristics (thermal conductivity and viscosity) through tube/channel. The selected coordinates are $\bar{x}$ and $\bar{y}$ which is taken along and perpendicular to the walls of the channel (Figure 1). The liquid is subjected to a transverse applied magnetic field (MF) B_1. Low Reynolds number approximation is used, and thus induced magnetic field (IMF) can be ignored. When the fluid moves into the MF, two important physical influences emerge. The initial one is that it causes an EF (electric field) in the stream. Assuming that there is no polarization charge thickness and, then, $\nabla.E_1 = 0$. Ignoring the IMF suggests that $\nabla \times E_1 = 0$, and in this way, the induced electric field is unimportant. The subsequent impact is progressively in nature, like a Lorentz or drag force $(J \times B_1)$, where J is the current density; this force follows up on the liquid and changes its movement. This result is in the exchange of energy between the field of electromagnetic and the fluid. In the current analysis, the relativistic impacts are ignored, and Ohm's law gives the current density J as [7]:

$$J = \sigma(V \times B_1) \tag{1}$$

where V is the field of velocity and σ the electrical conductivity. The liquid motion is created by the obligation of sinusoidal waves along the channel surface of the walls. The geometry of the wall is assumed by [6]:

$$\bar{y} = \pm H_0(\bar{x}, \bar{t}) = a_0 + b_0 \sin\left(2\pi\lambda^{-1}\left[\bar{x} - c\bar{t}\right]\right) \tag{2}$$

where a_0, b_0, c_0, λ and $\bar{t}$ signify the channel half-width, wave amplitude and as well as speed, wavelength and the temporal coordinate called time.

The dimensional equations of the governing flow problem in a laboratory frame of references (LFR) are given by [36]:

$$\frac{\partial \bar{u}}{\partial \bar{x}} + \frac{\partial \bar{v}}{\partial \bar{x}} = 0 \tag{3}$$

$$\rho\left(\frac{\partial \bar{u}}{\partial \bar{t}} + \bar{u}\frac{\partial \bar{u}}{\partial \bar{x}} + \bar{v}\frac{\partial \bar{u}}{\partial \bar{y}}\right) = -\frac{\partial \bar{p}}{\partial \bar{x}} + \frac{\partial \bar{\tau}_{\bar{x}\bar{x}}}{\partial \bar{x}} + \frac{\partial \tau_{\bar{x}\bar{y}}}{\partial \bar{y}} - \sigma B_0^2 \bar{u} \tag{4}$$

$$\rho\left(\frac{\partial \bar{v}}{\partial \bar{t}} + \bar{u}\frac{\partial \bar{v}}{\partial \bar{x}} + \bar{v}\frac{\partial \bar{v}}{\partial \bar{y}}\right) = -\frac{\partial \bar{p}}{\partial \bar{y}} + \frac{\partial \bar{\tau}_{\bar{x}\bar{x}}}{\partial \bar{x}} + \frac{\partial \tau_{\bar{x}\bar{y}}}{\partial \bar{y}} \tag{5}$$

$$\rho c_p\left(\frac{\partial \bar{T}}{\partial \bar{t}}+\bar{u}\frac{\partial \bar{T}}{\partial \bar{x}}+\bar{v}\frac{\partial \bar{T}}{\partial \bar{y}}\right)=k(\bar{T})\left(\frac{\partial^2 \bar{T}}{\partial \bar{x}^2}+\frac{\partial^2 \bar{T}}{\partial \bar{y}^2}\right)+\bar{\tau}_{\bar{x}\bar{x}}\frac{\partial \bar{u}}{\partial \bar{x}}+\bar{\tau}_{\bar{y}\bar{y}}\frac{\partial \bar{v}}{\partial \bar{y}}+\bar{\tau}_{\bar{x}\bar{y}}\left(\frac{\partial \bar{v}}{\partial \bar{x}}+\frac{\partial \bar{u}}{\partial \bar{y}}\right) \tag{6}$$

$$\left(\frac{\partial \bar{C}}{\partial \bar{t}}+\bar{u}\frac{\partial \bar{C}}{\partial \bar{x}}+\bar{v}\frac{\partial \bar{C}}{\partial \bar{y}}\right)=D_m\left(\frac{\partial^2 \bar{C}}{\partial \bar{x}^2}+\frac{\partial^2 \bar{C}}{\partial \bar{y}^2}\right)+\frac{D_m K_T}{T_m}\left(\frac{\partial^2 \bar{T}}{\partial \bar{x}^2}+\frac{\partial^2 \bar{T}}{\partial \bar{y}^2}\right) \tag{7}$$

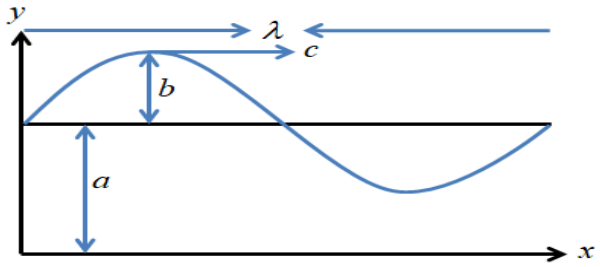

Figure 1. The geometry of the peristaltic wave in a channel

The flow is unsteady in the LFR. Let us consider the wave structure of references (x', y') with a uniform velocity c_0 , along with the variables corresponding to wave and LFR as:

$$x'=\bar{x}-c_0\bar{t}, y'=\bar{y}, u'=\bar{u}-c_0, v'=\bar{v} \text{ and } p(x')=\bar{p}(\bar{x},\bar{t}) \tag{8}$$

where $\bar{u},\bar{v},\rho,\bar{p},\sigma,B_0,D_m,K_T,T_m,c_p,k,\bar{T},\bar{C},\bar{\tau}_{\bar{x}\bar{y}},\bar{\tau}_{\bar{x}\bar{x}},\bar{\tau}_{\bar{y}\bar{y}}$ are called axial and transverse velocities, density, pressure, conductivity, the magnetic field strength, mass diffusivity of constant-coefficient, the thermal diffusion ratio, and mean liquid temperature, specific heat at uniform pressure, thermal conductivity, temperature, concentration, and extra stress components, respectively.

The governing flexible wall equations are defined as [27, 28]:

$$L(h_1)=-\left(p_0-p\right) \tag{9}$$

The operator L characterises the motion of the stretched membrane such that:

$$L=-\tau\frac{\partial^2}{\partial x^2}+n_1\frac{\partial^2}{\partial t_1^{\,2}}+n_2\frac{\partial}{\partial t_1}+n_3\frac{\partial^4}{\partial x^4}+H \tag{10}$$

where τ is the elastic tension, n_2 coefficient of wall damping force, H spring stiffness, n_3 rigidity of the plate and n_1 called the mass per unit area. Further, the p_0 on the exterior surface of the wall is negligible and hence consider $p_0=0$

The equation of continuity implies that at the surface of the fluid and the channel wall such as the pressure must be unique as that which acts on the liquid at the position $y=h_1$. By using the x component of momentum, the continuity equation at $y=h_1$ is given by:

$$\frac{\partial}{\partial x}(L(h_1))=\frac{\partial p}{\partial x}=\frac{\partial \tau_{x'x'}}{\partial x}+\frac{\partial \tau_{x'y'}}{\partial y}-\rho\left(\frac{\partial u}{\partial t}+u\frac{\partial u}{\partial x}+v_1\frac{\partial u}{\partial y}\right)-\sigma B_0^2 u \tag{11}$$

The governing equations are made dimensionless by utilizing the following non-dimensional parameters

$$x=\frac{x'}{\lambda},\ y=\frac{y'}{a_0},\ u=\frac{u'}{c_0},\ v=\frac{v'}{c_0\delta},\ h_1=\frac{H_0}{a_0},\ \delta=\frac{a_0}{\lambda},\ p=\frac{p'a_0^{\,2}}{\mu_0\lambda c_0},\ \mathrm{Re}=\frac{a_0c_0}{\vartheta},\ \vartheta=\frac{\mu_0}{\rho},$$
$$\tau_{xx}=\frac{a_0\tau'_{x'x'}}{\mu_0c_0},\tau_{xy}=\frac{a_0\tau'_{x'y'}}{\mu_0c_0},\tau_{yy}=\frac{a_0\tau'_{y'y'}}{\mu_0c_0},\ \psi'=\frac{\psi}{a_0c_0},\ \varepsilon=\frac{b_0}{a_0},\ t=\frac{t'c_0}{\lambda},\ E_1=\frac{-\tau a_0^{\,3}}{\lambda\mu_0^3c_0},\ \mathrm{Pr}=\frac{\mu_0c_p}{k_0},$$
$$E_2=\frac{n_1c_0a_0^{\,3}}{\lambda^3\mu_0},\ E_3=\frac{n_2a_0^{\,3}}{\lambda^3\mu_0},\ E_4=\frac{n_3a_0^{\,3}}{\lambda^5\mu_0c_0},\ E_5=\frac{H_0a_0^{\,3}}{\lambda\mu_0c_0},\ \mu_0'=\frac{\mu_0}{\mu},\ \theta=\frac{T_1-T_0}{T_0},Sc=\frac{\mu_0}{\rho D_m},$$
$$M=\sqrt{\frac{\sigma}{\mu_0}}B_0a_0,Ec=\frac{c_0^{\,2}}{c_pT_0},\sigma=\frac{C'-C_0}{C_0},Sr=\frac{\rho D_mK_TT_0}{T_m\mu C_0}. \tag{12}$$

The above Eq. (12) is used to non-dimensionalize the governing equations. Also, incorporating the small Reynolds number approximations and the long wavelength, the Eqs. (3)-(7) ease to the following :

$$\frac{\partial p}{\partial x}=\frac{\partial\tau_{xy}}{\partial y}-M^2(u+1) \tag{13}$$

$$\frac{\partial p}{\partial y}=0 \tag{14}$$

$$\frac{\partial}{\partial y}\left(k(\theta)\frac{\partial\theta}{\partial y}\right)+Br\,\tau_{x_1y_1}\left(\frac{\partial u}{\partial y}\right)=0 \tag{15}$$

$$\frac{\partial^2\sigma}{\partial y^2}+ScSr\frac{\partial^2\theta}{\partial y^2}=0 \tag{16}$$

where τ_{xy} is the governing equation of Bingham fluid and in the dimensionless form, it is given by,

$$\tau_{xy}=\mu(y)\frac{\partial u}{\partial y}+\tau_0 \tag{17}$$

where μ is the viscosity of the fluid and τ_0 denotes the stress.

The dimensionless slip appropriate boundary conditions (BCs) are given by:

$$u+\alpha\frac{\partial u}{\partial y}=-1,\ \theta+\beta\frac{\partial\theta}{\partial y}=0,\ \sigma+\gamma\frac{\partial\sigma}{\partial y}=0\ \text{ at }\ y=h_1=1+\varepsilon\sin\left[2\pi(x-t)\right] \tag{18}$$

$$\frac{\partial\sigma}{\partial y}=0,\frac{\partial\theta}{\partial y}=0,\frac{\partial u}{\partial y}=\tau_0\quad\text{at}\quad y=0 \tag{19}$$

where β,α and γ are the thermal and velocity slip and concentration slip, respectively.

Variable Liquid Properties

Most natural fluids have a distinction in thermophysical characteristics because of a healthy animal or biological comparable size will consistently take 1-2 liters of fluid. In the intestine, 6-7 liters are also found when it discharges from the salivary glands, pancreas, thyroid and liver. This involves dependence on the concentration of liquid along the x-axis, which causes the viscosity to decrease closer to the surface of the vessel. The k behaviour also varies according to temperature. Hence, the variations in viscosity and thermal conductivity are given by:

$$\begin{aligned}\mu(\mathrm{y})&=1-\alpha_1y,\quad\text{for}\ \ \alpha_1<<1,\\ k(\theta)&=\phi\theta+1,\quad\text{for}\ \ \phi<<1,\end{aligned} \tag{20}$$

where α_1,ϕ called the coefficients of variable viscosity and thermal conductivity, respectively.

SOLUTION METHODOLOGY

It is owing to the highly non-linearity in nature of the Eqs. (13) and (15), which are difficult to solve exactly. Thus, the perturbation method is implemented to spread the equation of the velocity u and temperature filed θ for the low values of α_1 and ϕ. However, the sealed or compact-form result is attained for the concentration from Eq. (16). Let,

$$u = u_0 + \alpha_1 u_1 + O(\alpha_1^2) \tag{21}$$

$$\theta = \theta_0 + \phi\theta_1 + O(\phi^2) \tag{22}$$

Substituting the Eq. (21) in Eq. (13) and doing exercise of the BCs (18) and (19), obtain the expressions for velocity from perturbation technique as

$$\begin{aligned} u = {} & \frac{1}{R_3}\left[R_1 - P\cosh(M\,y) + M\left(\alpha M\tau_0\cosh(M(y-h)) + R_2 - \tau_0\sinh(M(y-h))\right)\right] \\ & + \frac{\alpha_1 e^{-My}}{R_4}\left\{\begin{array}{l} P\left[R_5(y) + e^{2My}R_6(y)\right] + M\left[\begin{array}{l} R_7(-R_5(y)) - e^{2My}R_8R_6(y) \\ +16M^2\left(e^{2My}R_{17} + R_{18}\right)\end{array}\right]\cosh(hM) \\ +M\left[R_7R_5(y) + e^{2My}R_8R_6(y) + 16\alpha M^3\left(e^{2My}R_{17} + R_{18}\right)\right]\sinh(hM)\end{array}\right\} \end{aligned} \tag{23}$$

Where

$R_1 = -(M^2+P)\cosh(hM), R_2 = \alpha(M^2+P)\sinh(hM), R_3 = M^2(\cosh(hM) + aM\sinh(hM)),$

$R_4 = 16MR_3, R_5(y) = 1-2M\,y(-1+M\,y), R_6(y) = -1+2M\,y(1+M\,y), R_7 = (1+\alpha M)\tau_0,$

$R_8 = (-1+\alpha M)\tau_0, R_9 = \left[(8+\alpha)\tau_0 + 8MR_{18}\right]\cosh(hM), R_{10} = (\tau_0 + 8\alpha M^2 + 8\alpha M^3 R_{18})\sinh(hM),$

$R_{11} = 8M^3(-1+\alpha M) - P, R_{12} = \left(\alpha + 2h - 2h(3\alpha+h)M + 2\alpha h^2M^2\right)P, R_{13} = 8M^3(1+\alpha M),$

$R_{14} = M(1+8M)(1+\alpha M)\tau_0, R_{15} = 3 + M\left(-8 + M\left(\begin{array}{l}-8\alpha h - 4h^2 + \alpha^2 \\ \left(1+4M\left(2+h^2M\right)\right)\end{array}\right)\right),$

$R_{16} = 8M^3\left(1-\alpha M + e^{2hM}(1+\alpha M)\right)^2, R_{17} = \dfrac{-P + M^2(R_9 + MR_{10})}{8MR_3},$

$R_{18} = \dfrac{1}{R_{16}}\left(e^{Mh}\left(R_{11} - MR_{12} - e^{2hM}\left(R_{13} + R_{14}P\right) - e^{3hM}R_{14} + e^{hM}MR_{15}\tau_0\right)\right).$

Here nothing just the x-component of P looking in Eq. (23) and well-defined by Eq. (11) is further ease as follows:

$$P = 8\varepsilon\pi^3\left(\frac{-0.5E_3}{\pi}\sin 2\pi(t-x) - \left[E_1 + E_2 - 4\pi^2E_4 - \frac{0.25E_5}{\pi^2}\right]\cos 2\pi(t-x)\right)$$

The flow pattern function will be established by integrating Eq. (23) with the condition $\psi = 0$ at $y = 0$. Following the same procedure, the expression for temperature and concentration can be obtained from Eqs. (15) and (16) after performing lengthy calculations.

Validation of the model

In view of a realistic approach to biological systems, the current paper aims at extending the results of Akram et al. [36] by incorporating the variable liquid properties, wall porosity, and slip conditions. The outcomes of the model developed in this paper are found to be in accordance with their results. Precisely, in the absence of velocity slip and variable viscosity parameter, the expression for the velocity field coincides with the result obtained by [36]. From this study, the influence of M on the velocity field can control blood flow during the surgeries because an upsurge in the magnetic field results in the reduction of velocity, which implies that blood flow will be trapped by varying the strength of magnetic. This result may help the doctors during the surgeries to reduce the flow of blood.

RESULTS AND DISCUSSIONS

This portion includes the effects of variable viscosity parameter (α_1) variable thermal conductivity parameter (ϕ), thermal and velocity slip constraints (α, β), concentration slip parameter (γ), Brinkmannand Schmidt number (Br, Sc), Soret number (Sr), the wall tension parameter (E_1), the mass characterization (E_2), the wall damping parameter (E_3), the rigidity parameter (E_4), and the wall elastic parameter (E_5) on the velocity (w), concentration (σ) ,temperature (θ) and as well as the streamlines (ψ) are analysed and deliberated through graphs 2-13. Moreover, the Matlab solver has been employed for the illustrative representations and to analyse the effects of the relevant constraints of the engineering quantities of interest on the physical aspects for the fixed values of the constraints are the following as for the whole computations of the paper $E_1 = 0.1, E_2 = 0.04, E_3 = 0.4, E_5 = 0.01,$ $E_4 = t = 0.1, \beta = 0.2, \alpha = 0.2, \tau_0 = 0.002, \gamma = 0.2, Br = 2, Sc = 0.2, Sr = 0.3, x = 0.2, \varepsilon = 0.6, \alpha_1 = 0.02, M = 1$ and $\phi = 0.02$

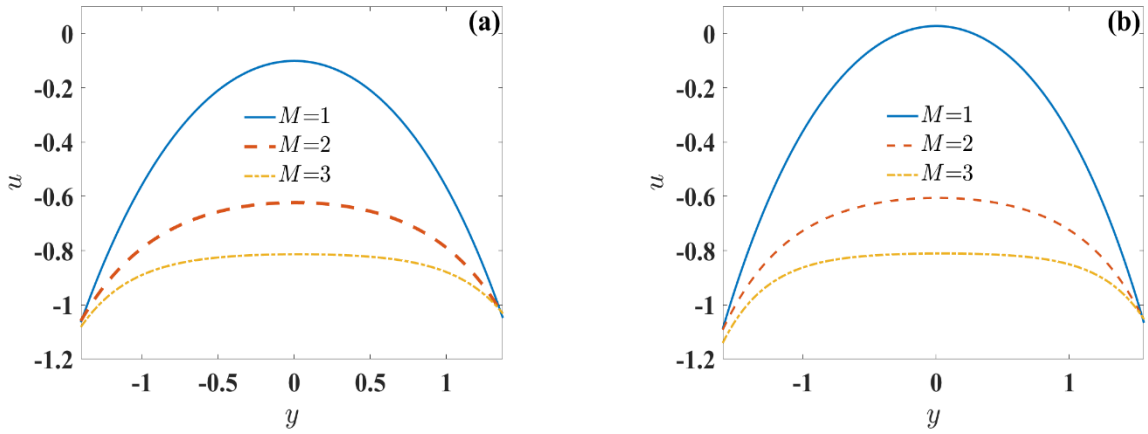

Figure 2. The profiles of velocity for varying magnetic parameter (M) when (a) $\alpha = 0$ and (b) $\alpha = 0.2$

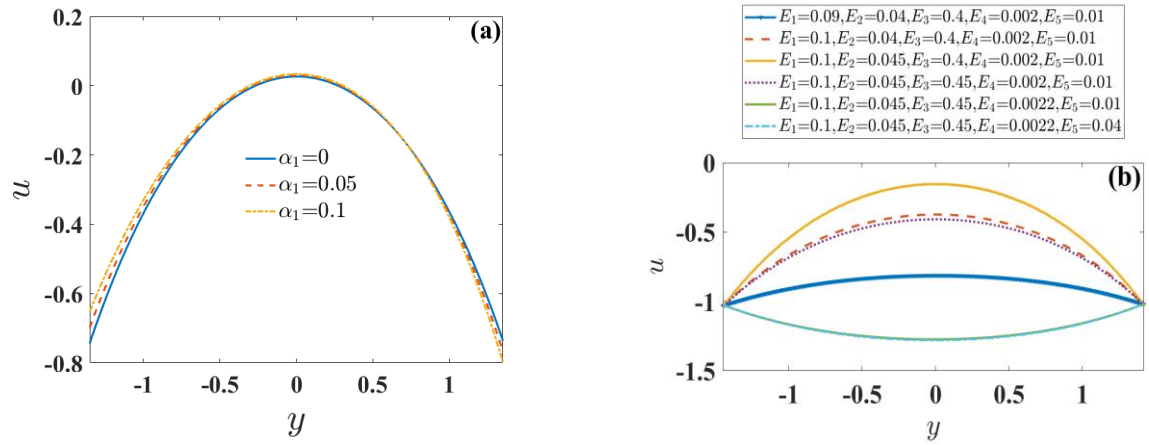

Figure 3. Velocity profiles for varying (a) variable viscosity (α_1) and (b) wall properties $(E_1 - E_5)$

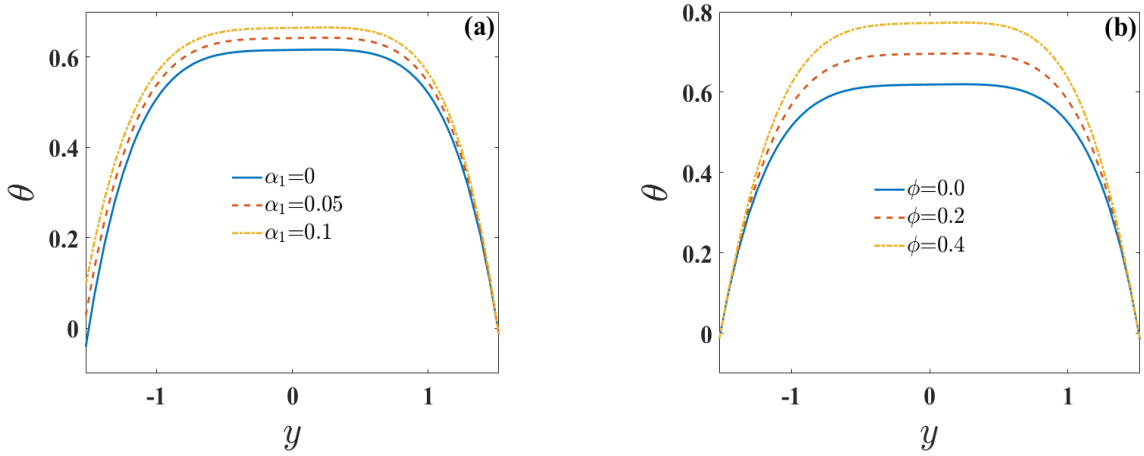

Figure 4. Temperature profiles for changing (a) variable viscosity (α_1) and (b) variable thermal conductivity (ϕ)

Velocity fields

Figures 2 and 3 show the variations of M, α, α_1, E_3, E_4, E_1, E_2 and E_5 on the field of velocity. From these figures, it is clear that the extreme velocity occurs in the central region in which outcomes are in a parabolic trajectory. Figure 2 shows the stimulus of magnetization on the velocity profiles for specific magnetic and slip parameter values is demonstrated. The aforementioned figure shows that the Hartmann number moderates the fluid flow (see Figure 2(a)). This action is evident since the flow resists the transverse magnetic field. The transverse magnetic field, especially in blood, results in rouleaux forming, leading to a reduction in the field of velocity. Further, it is also noticed that the fluid flows rapidly due to upsurging in (Figure 2(b)). The impacts of variable viscosity and amplitude ratio on the field of velocity are depicted in Figure 3. The effect of variable viscosity outcomes in enhancing the velocity profiles in the center of the channel, but it is found to behave quite the opposite behaviour at the walls of the channel (Figure 3(a)). Illustration of 3(b) represents the variability in the velocity field of the wall properties. It is perceived that the flows of the liquid is going quickly with augmenting the values selection of E_1 and E_2 and the flow is retarded for growingideals of E_4, E_3 and E_5.

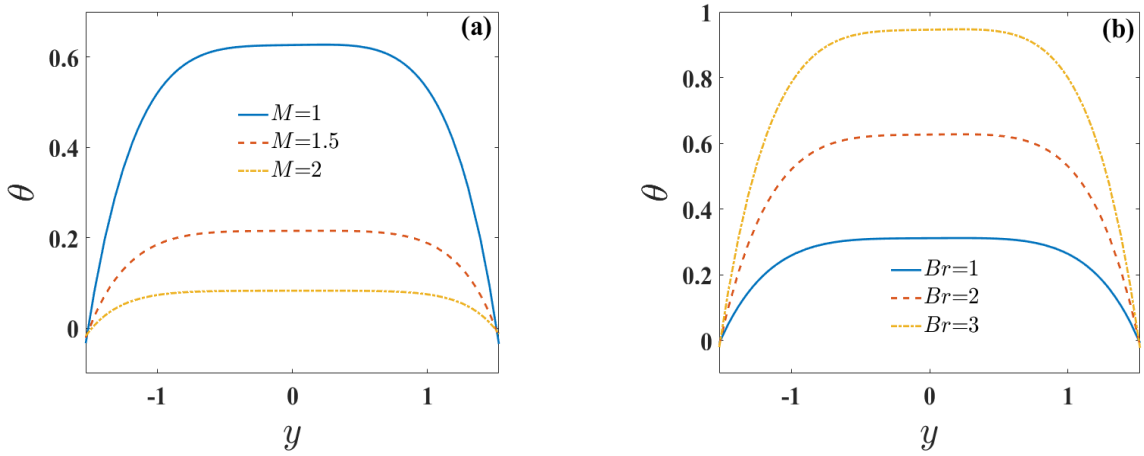

Figure 5. Temperature profiles for varying (a) magnetic parameter (M) and (b) Brinkmann number (ϕ)

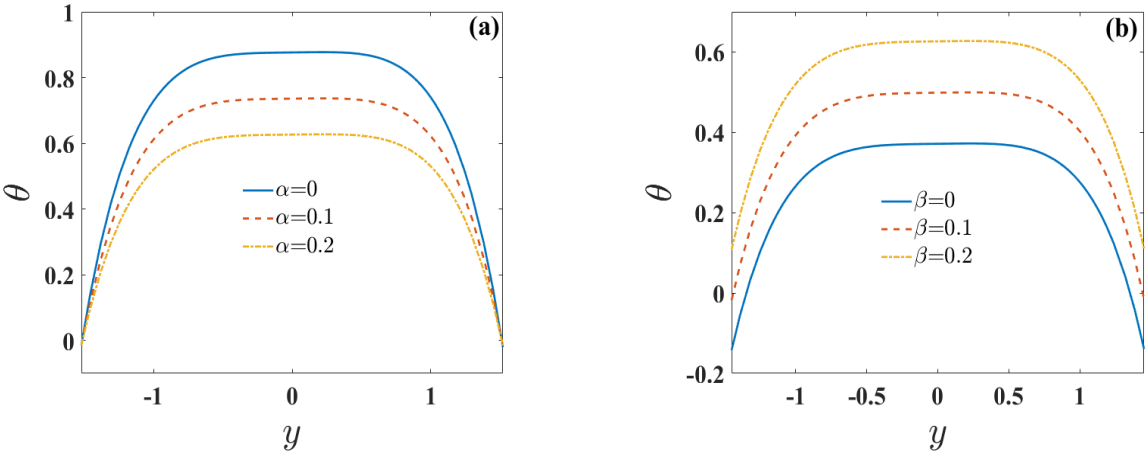

Figure 6. Temperature profiles for varying (a) velocity slip parameter (α) and (b) thermal slip parameter (β)

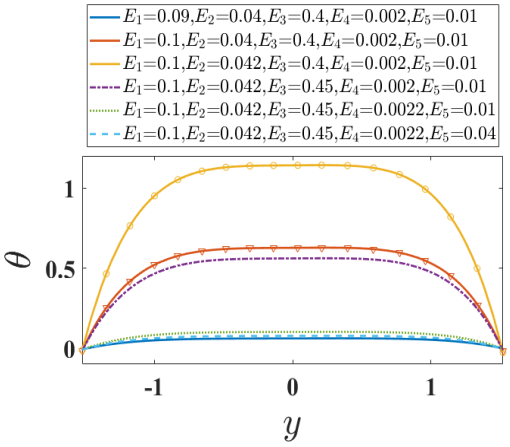

Figure 7. Temperature profiles for varying wall parameters $(E_1 - E_5)$

Temperature Profiles

The deviations of α_1, ϕ, M, Br, α, β, E_1, E_2, E_3, E_4 and E_5 on the temperature field are inspected in Figures 4 to 7. In the core part the fluid temperature increases leading to a parabolic curve. The deviation of viscous dissipation (VD) on the temperature profiles will contemplate this character of the graph. The viscous dissipation happens by means of fluid viscosity, leading to the change of kinetic energy into internal thermal energy. The impacts on temperature profiles of α_1 and ϕ are described in Figure 4. Figure 4(a) depicts the increasing upshot of α_1 on temperature plot. This is because of an increment in the α_1 of the fluid results in diminishing the heat transfer capacity. Further, larger values of k enhance the fluid temperature (See Figure 4(b)). However, the fluid k delivers the indication of the liquid's ability to maintain or expel the heat around it. Thus, whenever the fluid's k bonded within the channel is greater than the wall of the temperature. Figure 5 portrays the effects of the M and Br on the temperature profiles. The decreasing influence of Hartmann number on θ is realised in Figure 5(a). The opposite behaviour is noticed for a rise in the Brinkmann number Figure (5(b)). This is recognised to the increase in the flow resistance due to a rise in the value of the Br, which causes the VD effects to inflate the thermal energy internally. You can see the contrary impact of speed parameters and thermal slip parameters in Figures 6(a) and 6(b), in which the temperature decreases with the α and the β increases. From Figure 7, it is noticed that the θ enhance for growing values of E_1 and E_2, whereas a contradictory tendency is noticed with E_3, E_4 and E_5.

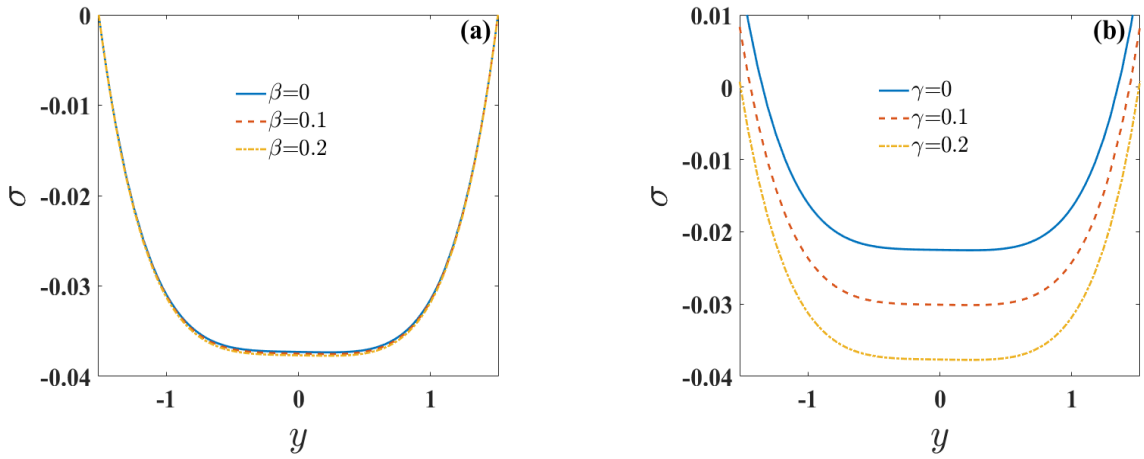

Figure 8. Concentration profiles for varying (a) thermal slip parameter (β) and (b) concentration slip parameter (γ)

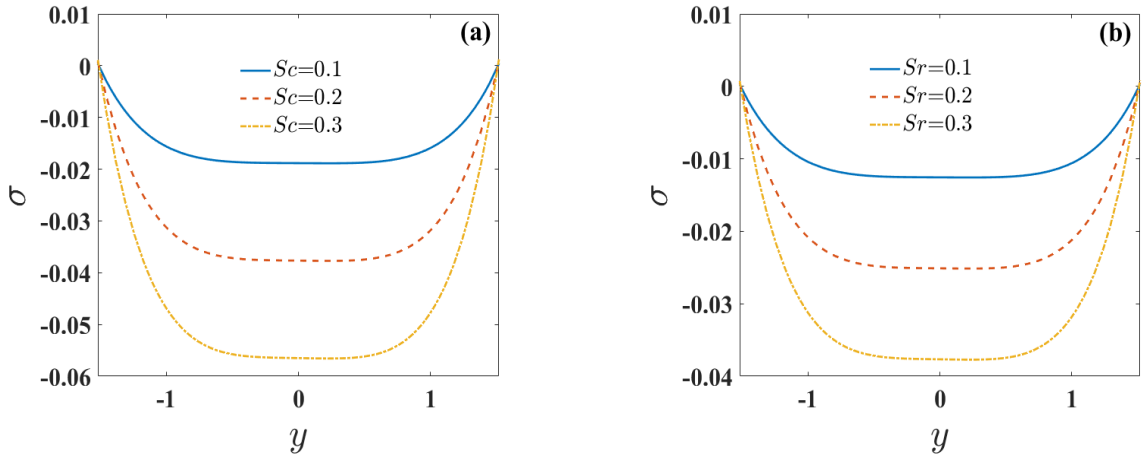

Figure 9. Concentration profiles for varying (a) Schmidt number (Sc) and (b) Soret number (Sr)

Concentration profiles

The σ reveal the opposing impact as compared with the θ. This behavior is logically rational because heat and mass are understood to have an inverse relationship. It is also evident from patterns that particles of a liquid are more stucked near the channel of the wall than in the dominant area. This activity becomes apparent biologically and plays the vital nutrients from the blood compared to the other fluid's disperse to neighboring cells and tissues. Figures 8 and 9 is used to highlight the impact of β, γ, Sc and Sr on the σ. Here, an upsurge in the choices of β, γ, Sc and Sr reduces the temperature profiles.

Trapping phenomenon

Trapping is a fascinating process in indulgent the flow patterns of biological liquids such as thrombus flow of blood in vessels, movement of chyme in the gastrointestinal tract. The process of peristaltic involved in these systems especially allows us to examine the movement and making of the bolus. The volume of the stuck bolus is originated to fall with M and α (See Figures 10 and 11). The influence of variable viscosity constraint improves the size of the stuck bolus (Figure 12). Figure 13 demonstrates the variation of wall features on the stuck bolus. Here, aincrease in the values of E_1 and E_2 increases the size of the stuck bolus, whereas quite the opposite behaviour is noticed with E_3, E_4 and E_5.

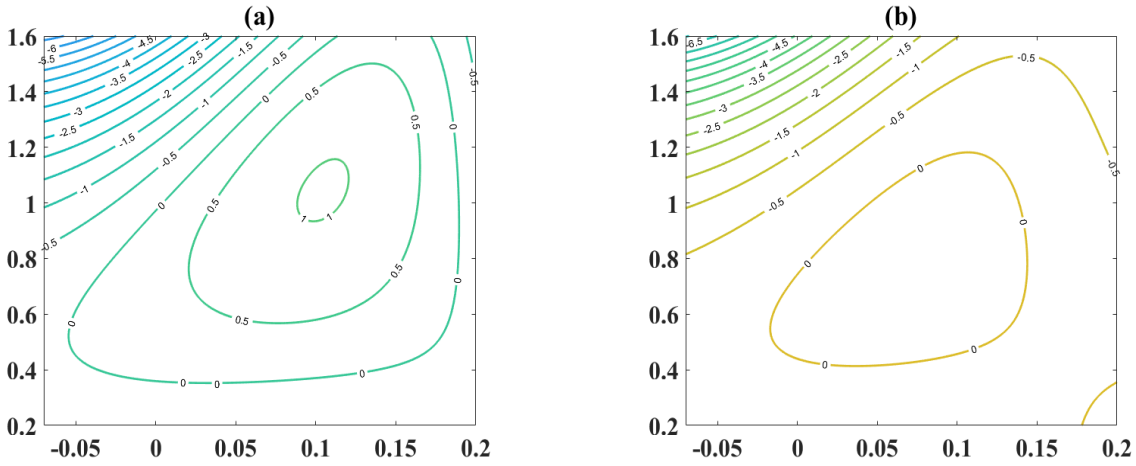

Figure 10. Streamlines for varying magnetic parameter (M) when (a) $M = 1$ and (b) $M = 2$

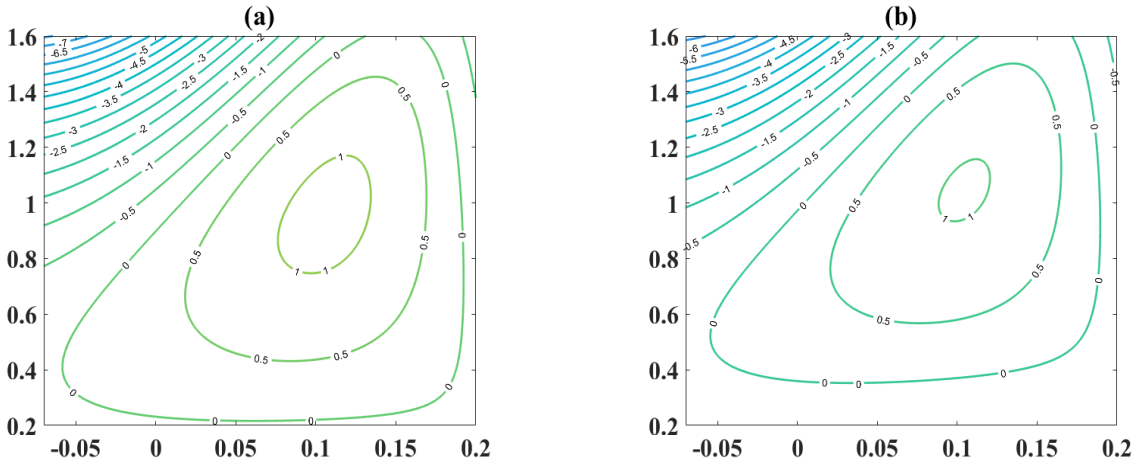

Figure 11. Streamlines for varying velocity slip parameter (α) when (a) $\alpha = 0.1$ and (b) $\alpha = 0.2$

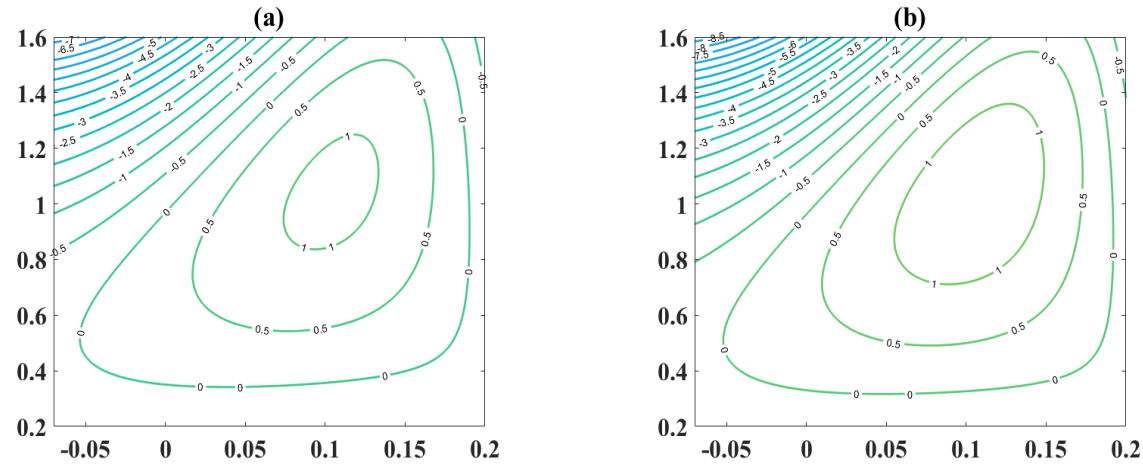

Figure 12. Streamlines for varying variable viscosity (α_1) when (a) $\alpha_1 = 0.1$ and (b) $\alpha_1 = 0.3$

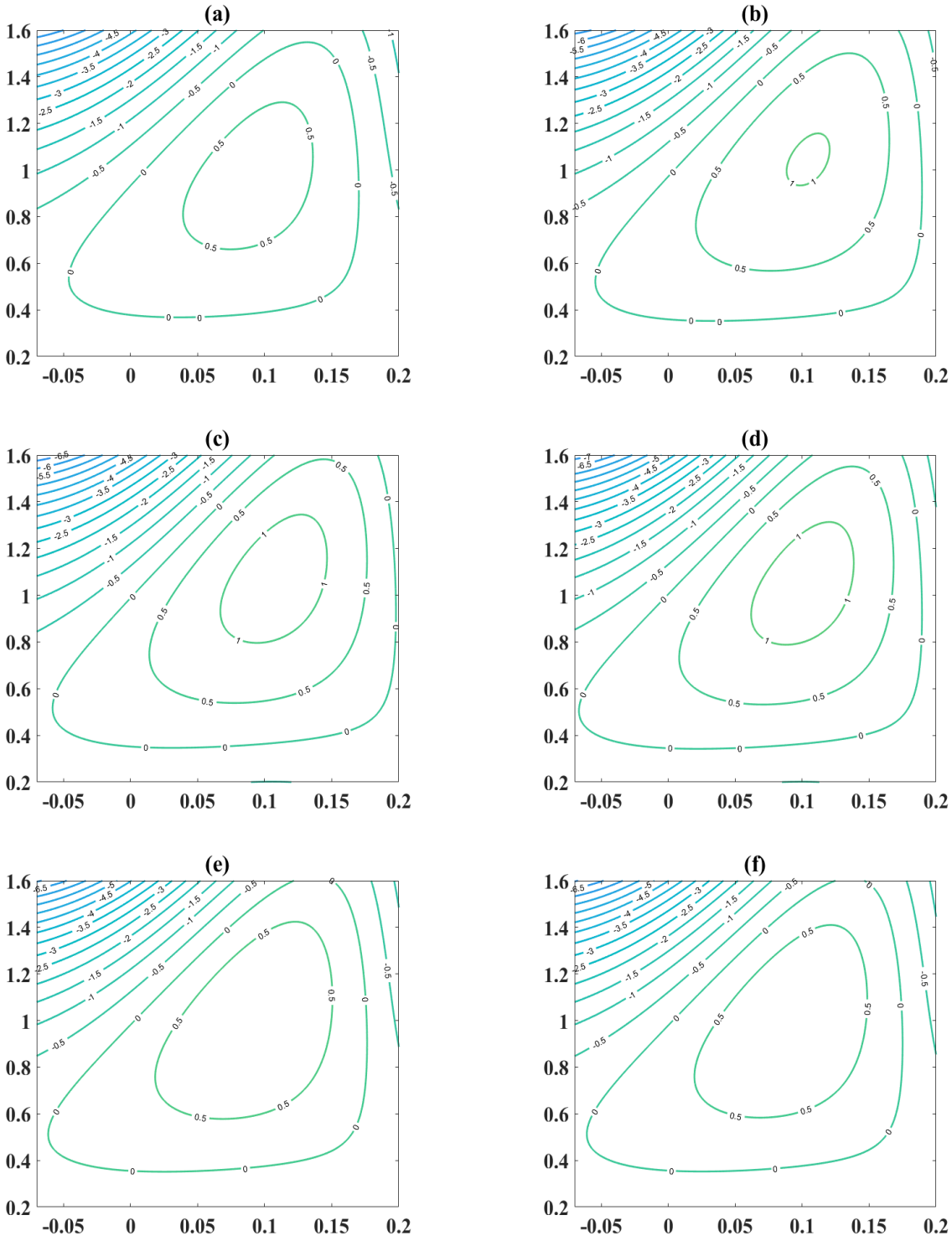

Figure 13. Streamlines for varying variable viscosity (α_1) when (a) $E_1 = 0.08, E_2 = 0.03, E_3 = 0.3, E_4 = 0.001, E_5 = 0.02$, (b) $E_1 = 0.1, E_2 = 0.03, E_3 = 0.3, E_4 = 0.001, E_5 = 0.02$, (c) $E_1 = 0.1, E_2 = 0.035, E_3 = 0.3, E_4 = 0.001, E_5 = 0.02$, (d) $E_1 = 0.1, E_2 = 0.035, E_3 = 0.35, E_4 = 0.001, E_5 = 0.02$, (e) $E_1 = 0.1, E_2 = 0.035, E_3 = 0.4, E_4 = 0.001, E_5 = 0.02$ and (f) $E_1 = 0.1, E_2 = 0.035, E_3 = 0.4, E_4 = 0.001, E_5 = 0.5$.

CONCLUSIONS

This article examines the impacts of variable liquid characteristics on the MHD peristaltic process. The effects of heat and mass exchange are contemplated through a constant channel affected by slip and wall properties. Plots describe the

variations of specific constraints on the interest-bearing physiological quantities. The important points of the current article can be summarized as:

1. The velocity and temperature profiles increase in the presence of variable viscosity. The Hartmann number shows a drop behaviour in the velocity profiles.
2. The augmentation in velocity and temperature is detected, respectively, for an upsurge in the values of β and α.
3. The temperature and the velocity field can be upsurges owing to increasing the mass characterization and wall tension parameters.
4. The profiles of concentration demonstrate the opposite trend as relative to the θ.
5. The Sr and as well as Sc decelerated in the field of concentration.
6. The drop in the bolus formation is noticed for a rise in the magnetic and velocity slip parameters.

REFERENCES

[1] T. W. Latham, "Fluid motions in a peristaltic pump." 1966.

[2] K. . Raju and R. Devantahan, "Peristaltic trasport of non-Newtonian fluid," *Rheol. Acta*, vol. 11, pp. 170–178, 1972.

[3] S. Nadeem and S. Akram, "Peristaltic Flow of a Maxwell Model Through Porous Boundaries in a Porous Medium," *Transp. Porous Media*, vol. 86, no. 3, pp. 895–909, 2011, doi: 10.1007/s11242-010-9663-z.

[4] G. Böhme and A. Müller, "Analysis of non-Newtonian effects in peristaltic pumping," *J. Nonnewton. Fluid Mech.*, vol. 201, pp. 107–119, 2013, doi: 10.1016/j.jnnfm.2013.08.002.

[5] M. G. Reddy, B. C. Prasannakumara, and O. D. Makinde, "Cross diffusion impacts on hydromagnetic radiative peristaltic carreau-casson nanofluids flow in an irregular channel," *Defect Diffus. Forum*, vol. 377, pp. 62–83, 2017, doi: 10.4028/www.scientific.net/DDF.377.62.

[6] C. Rajashekhar, G. Manjunatha, K. V Prasad, B. B. Divya, and H. Vaidya, "Peristaltic transport of two-layered blood flow using Herschel-Bulkley Model ," *Cogent Eng.*, vol. 5, p. 1495592, 2017, doi: 10.1080/23311916.2018.1495592.

[7] S. Nadeem and S. Akram, "Heat transfer in a peristaltic flow of MHD fluid with partial slip," *Commun. Nonlinear Sci. Numer. Simul.*, vol. 15, no. 2, pp. 312–321, 2010, doi: 10.1016/j.cnsns.2009.03.038.

[8] N. S. Akbar and S. Nadeem, "Thermal and velocity slip effects on the peristaltic flow of a six constant Jeffrey's fluid model," *Int. J. Heat Mass Transf.*, vol. 55, no. 15–16, pp. 3964–3970, 2012, doi: 10.1016/j.ijheatmasstransfer.2012.03.026.

[9] R. Latha, B. R. Kumar, and O. D. Makinde, "Peristaltic flow of couple stress fluid in an asymmetric channel with partial slip," *Defect Diffus. Forum*, vol. 387, pp. 385–402, 2018, doi: 10.4028/www.scientific.net/DDF.387.385.

[10] A. Wakif, Z. Boulahia, S. R. Mishra, M. Mehdi Rashidi, and R. Sehaqui, "Influence of a uniform transverse magnetic field on the thermo-hydrodynamic stability in water-based nanofluids with metallic nanoparticles using the generalized Buongiorno's mathematical model," *Eur. Phys. J. Plus*, vol. 133, no. 5, 2018, doi: 10.1140/epjp/i2018-12037-7.

[11] B. Mahanthesh, G. Lorenzini, F. M. Oudina, and I. L. Animasaun, "Significance of exponential space- and thermal-dependent heat source effects on nanofluid flow due to radially elongated disk with Coriolis and Lorentz forces," *J. Therm. Anal. Calorim.*, vol. 141, no. 1, pp. 37–44, 2020, doi: 10.1007/s10973-019-08985-0.

[12] S. Hamrelaine, F. Mebarek-Oudina, and M. R. Sari, "Analysis of MHD Jeffery Hamel flow with suction/injection by homotopy analysis method," *J. Adv. Res. Fluid Mech. Therm. Sci.*, vol. 58, no. 2, pp. 173–186, 2019.

[13] F. Mebarek-Oudina, "Convective heat transfer of Titania nanofluids of different base fluids in cylindrical annulus with discrete heat source," *Heat Transf. - Asian Res.*, vol. 48, no. 1, pp. 135–147, 2019, doi: 10.1002/htj.21375.

[14] S. S. J. Raza, F. Mebarek-Oudina, P. Ram, "MHD flow of non-Newtonian molybdenum disulfide nanofluid in a converging/diverging channel with Rosseland radiation," *Defect Diffus. Forum*, vol. 401, pp. 92–106, 2020.

[15] S. Marzougui, F. Mebarek-Oudina, A. Assia, M. Magherbi, Z. Shah, and K. Ramesh, "Entropy generation on magneto-convective flow of copper–water nanofluid in a cavity with chamfers," *J. Therm. Anal. Calorim.*, vol. 143, no. 3, pp. 2203–2214, 2021, doi: 10.1007/s10973-020-09662-3.

[16] X. Guo, J. Zhou, H. Xie, and Z. Jiang, "MHD peristaltic flow of fractional Jeffrey model through porous medium," *Math. Probl. Eng.*, vol. 2018, 2018, doi: 10.1155/2018/6014082.

[17] T. Hayat, H. Zahir, A. Tanveer, and A. Alsaedi, "Soret and Dufour effects on MHD peristaltic flow of Prandtl fluid in a rotating channel," *Results Phys.*, vol. 8, pp. 1291–1300, 2018, doi: 10.1016/j.rinp.2018.01.058.

[18] A. Tanveer, T. Hayat, and A. Alsaedi, "Peristaltic flow of MHD Jeffery nanofluid in curved channel with convective boundary conditions: a numerical study," *Neural Comput. Appl.*, vol. 30, no. 2, pp. 437–446, 2018, doi: 10.1007/s00521-016-2705-x.

[19] K. A. Kumar, B. Ramadevi, V. Sugunamma, and J. V. R. Reddy, "Heat transfer characteristics on MHD Powell-Eyring fluid flow across a shrinking wedge with non-uniform heat source/sink," *J. Mech. Eng. Sci.*, vol. 13, no. 1, pp. 4558–4574, 2019, doi: 10.15282/jmes.13.1.2019.15.0385.

[20] G. Manjunatha, C. Rajashekhar, H. Vaidya, K. V. Prasad, O. D. Makinde, and J. U. Viharika, "Impact of Variable Transport Properties and Slip Effects on MHD Jeffrey Fluid Flow Through Channel," *Arab. J. Sci. Eng.*, vol. 45, no. 1, pp. 417–428, Jan. 2020, doi: 10.1007/s13369-019-04266-y.

[21] T. Hayat, M. U. Qureshi, and N. Ali, "The influence of slip on the peristaltic motion of a third order fluid in an asymmetric channel," *Phys. Lett. Sect. A Gen. At. Solid State Phys.*, vol. 372, no. 15, pp. 2653–2664, 2008, doi: 10.1016/j.physleta.2007.12.049.

[22] C. Rajashekhar, G. Manjunatha, H. Vaidya, B. B. Divya, and K. V. Prasad, "Peristaltic Flow of Casson Liquid in an Inclined Porous Tube with Convective Boundary Conditions and Variable Liquid Properties," *Front. Heat Mass Transf.*, vol. 11, Nov. 2018, doi: 10.5098/hmt.11.35.

[23] G. Manjunatha, C. Rajashekhar, H. Vaidya, K. V. Prasad, and O. D. Makinde, "Effects Wall Properties on Peristaltic Transport of Rabinowitsch Fluid through an Inclined Non-Uniform Slippery Tube," *Defect Diffus. Forum*, vol. 392, pp. 138–157, Apr. 2019, doi: 10.4028/www.scientific.net/DDF.392.138.

[24] G. Manjunatha, H. Vaidya, C. Rajashekhar, and K. V. Prasad, "Peristaltic Flow of a Jeffery Fluid with Heat Transfer in an Inclined Porous Tube under the Influence of Slip and Variable Viscosity," *Defect Diffus. Forum*, vol. 393, pp. 16–30, Jun. 2019, doi: 10.4028/www.scientific.net/DDF.393.16.

[25] G. Manjunatha, C. Rajashekhar, H. Vaidya, and K. V. Prasad, "Simultaneous effects of heat transfer and variable viscosity on peristaltic transport of Casson fluid flow in an inclined porous tube," *Int. J. Appl. Mech. Eng.*, vol. 24, no. 2, pp. 309–328, May 2019, doi: 10.2478/ijame-2019-0020.

[26] A. Bouaffane and K. Talbi, "Thermal study of fluid flow inside an annular pipe filled with porous media under local thermal non-equilibrium condition," *J. Mech. Eng. Sci.*, vol. 13, no. 2, pp. 4880–4897, 2019.

[27] S. Srinivas, R. Gayathri, and M. Kothandapani, "The influence of slip conditions, wall properties and heat transfer on MHD peristaltic transport," *Comput. Phys. Commun.*, vol. 180, no. 11, pp. 2115–2122, 2009, doi: 10.1016/j.cpc.2009.06.015.

[28] T. Hayat, M. Javed, and N. Ali, "MHD peristaltic transport of a Jeffery fluid in a channel with compliant walls and porous space," *Transp. Porous Media*, vol. 74, no. 3, pp. 259–274, 2008, doi: 10.1007/s11242-007-9196-2.

[29] M. Javed, T. Hayat, and A. Alsaedi, "Peristaltic flow of Burgers' fluid with compliant walls and heat transfer," *Appl. Math. Comput.*, vol. 244, pp. 654–671, 2014, doi: 10.1016/j.amc.2014.07.009.

[30] N. S. Gad, "Effects of hall currents on peristaltic transport with compliant walls," *Appl. Math. Comput.*, vol. 235, pp. 546–554, 2014, doi: 10.1016/j.amc.2014.02.081.

[31] M. Lachiheb, "Effect of coupled radial and axial variability of viscosity on the peristaltic transport of Newtonian fluid," *Appl. Math. Comput.*, vol. 244, pp. 761–771, 2014, doi: 10.1016/j.amc.2014.07.062.

[32] M. Lachiheb, "On the effect of variable viscosity on the peristaltic transport of a Newtonian fluid in an asymmetric channel," *Can. J. Phys.*, vol. 94, pp. 320–327, 2016.

[33] M. Awais, U. Bukhari, A. Ali, and H. Yasmin, "Convective and peristaltic viscous fluid flow with variable viscosity," *J. Eng. Thermophys.*, vol. 26, no. 1, pp. 69–78, 2017, doi: 10.1134/S1810232817010088.

[34] B. B. Divya, G. Manjunatha, C. Rajashekhar, V. Hanumesh, and K. V. Prasad, "Impact of variable liquid properties on peristaltic mechanism of convectively heated Jeffrey fluid in a slippery elastic tube," *Front. Heat Mass Transf.*, vol. 12, Apr. 2019, doi: 10.5098/hmt.12.15.

[35] H. Vaidya, C. Rajashekhar, G. Manjunatha, and K. V. Prasad, "Peristaltic mechanism of a Rabinowitsch fluid in an inclined channel with complaint wall and variable liquid properties," *J. Brazilian Soc. Mech. Sci. Eng.*, vol. 41, no. 1, p. 52, Jan. 2019, doi: 10.1007/s40430-018-1543-4.

[36] S. Akram, S. Nadeem, and A. Hussain, "Effects of heat and mass transfer on peristaltic flow of a Bingham fluid in the presence of inclined magnetic field and channel with different wave forms," *J. Magn. Magn. Mater.*, vol. 362, pp. 184–192, 2014, doi: 10.1016/j.jmmm.2014.02.063.

[37] L. Fusi and A. Farina, "Peristaltic axisymmetric flow of a Bingham fluid," *Appl. Math. Comput.*, vol. 320, pp. 1–15, 2018, doi: 10.1016/j.amc.2017.09.017.

[38] G. Manjunatha, C. Rajashekhar, H. Vaidya, and K. V. Prasad, "Peristaltic mechanism of Bingham liquid in a convectively heated porous tube in the presence of variable liquid properties," *Spec. Top. Rev. Porous Media An Int. J.*, vol. 10, no. 2, pp. 187–201, 2019, doi: 10.1615/SpecialTopicsRevPorousMedia.2019026973.

[39] H. Vaidya, C. Rajashekhar, G. Manjunatha, K. V Prasad, O. D. Makinde, and K. Vajravelu, "Heat and mass transfer analysis of MHD peristaltic flow through a complaint porous channel with variable thermal conductivity," *Phys. Scr.*, vol. 95, no. 4, p. 045219, Apr. 2020, doi: 10.1088/1402-4896/ab681a.

[40] R. Choudhari, M. Gudekote, H. Vaidya, K. V. Prasad, and S. U. Khan, "Rheological effects on peristaltic transport of Bingham fluid through an elastic tube with variable fluid properties and porous walls," *Heat Transf.*, vol. 49, no. 6, pp. 3391–3408, 2020, doi: 10.1002/htj.21779.